

# Elastic Instabilities of Polymer Solutions in Extensional Flows

P.E. Arratia<sup>1</sup>, C.C. Thomas<sup>1</sup>, J.D. Diorio<sup>1</sup>, and J.P. Gollub<sup>1,2</sup>

<sup>1</sup>*Department of Physics, Haverford College, Haverford, PA 19041*

<sup>2</sup>*Department of Physics, University of Pennsylvania, Philadelphia, PA 19104*

(Dated: November 16, 2005)

When polymer molecules pass near the hyperbolic point of a microchannel cross flow, they are strongly stretched. As the strain rate is varied at low Reynolds number, the stretching produces two flow instabilities, one in which the velocity field becomes strongly asymmetric, and a second in which it fluctuates non-periodically in time. The flow is strongly perturbed even far from the region of instability, and this phenomenon can be used to produce mixing.

PACS numbers: 47.50.+d, 83.60.Wc, 05.45.-a, 83.50.-v

The rheology of polymeric fluids is often complex, and their material properties have a strong impact on flow behavior. It has long been observed that the presence of polymer molecules in a fluid can lead to flow instabilities and non-linear dynamics [1-8]. For example, Giesekus [3] observed a cellular instability of a non-Newtonian fluid in Taylor-Couette flows, analogous to the classical Taylor-Couette instability of Newtonian fluids, but at very low Reynolds (Taylor) numbers. Later, Larson, Shaqfeh and Muller [9] demonstrated that such non-Newtonian instabilities can be driven solely by fluid elasticity. Recently, Groisman and Steinberg [10] demonstrated an increased flow resistance and other features of turbulence in polymeric fluids at very low Reynolds numbers ( $Re$ ). They find that viscoelasticity can enhance mixing in small curved channels [11].

Macroscopic non-Newtonian behavior results from microscopic stresses due to flow-induced changes in polymer conformation in solution. These stresses depend on the nature of the flow. Elongational (or extensional) flows, such as the flow in a cross-channel with two inputs and two outputs, can stretch and orient polymer molecules to a greater extent than ordinary shear flows [12]. The stresses due to polymer extension surely affect the flow and might lead to instabilities that are distinct from those observed in other geometries.

The behavior of polymers in extensional flows has received growing attention [13-16]. In particular, it has been suggested that elongational material properties may lead to fluid instabilities [8, 15]. Theoretical investigations [17, 18] predict that a flexible polymer molecule that is initially coiled at rest can be fully stretched if subjected to uniaxial extensional flow at sufficiently high strain rates. This is the so-called 'coil-stretch' transition, which is predicted to occur at  $\dot{\epsilon} = 0.5\lambda^{-1}$  [19], where  $\lambda$  is the relaxation time of the fluid and  $\dot{\epsilon}$  is the strain rate. Early experiments in cross-channel geometry using birefringence showed that molecules are extended in large strain fields, and that they align with the flow [20-22, 16]. More recently, experiments capable of imaging individual polymer molecules (DNA) near the stagnation point in a cross-channel flow [13, 23] found evidence of a sharp hysteretic transition from the coiled to the stretched state [24]. At high strain rates, however,

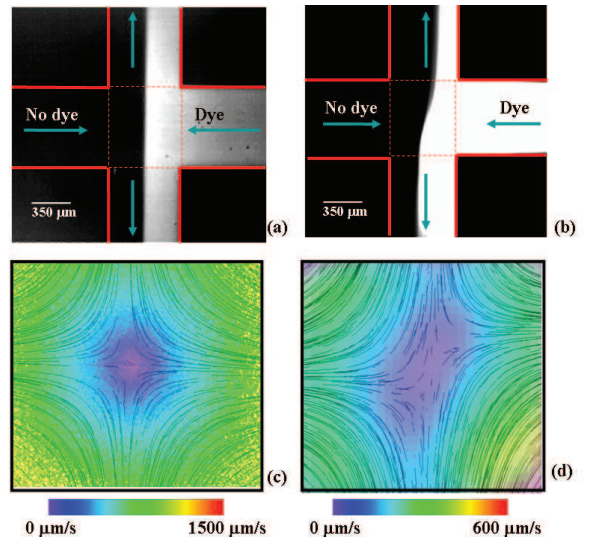


FIG. 1: (Color Online) Dye advection patterns for a cross channel flow with two inputs and two outputs (both at  $De=1.5$ ) for (a) Newtonian fluid, and (b) PAA flexible polymer solution, where the interface between dyed and undyed fluid is deformed by an instability. (c,d) particle streaklines and velocity field magnitudes corresponding to (a,b).

distinct molecular conformations with different dynamics were observed. An important question is how polymer molecules that are driven away from equilibrium affect the bulk flow behavior in a simple extensional flow.

In this Letter, we report two novel flow instabilities of a planar extensional flow of a dilute flexible polymer solution under steady forcing. In the first instability, the flow becomes deformed and asymmetric but remains steady. In a further instability that occurs at higher strain rates, the velocity field fluctuates non-periodically in time and can produce mixing. Newtonian and dilute stiff polymer solutions (not shown) are devoid of instabilities under these conditions (low  $Re$ ).

An extensional flow is generated in a flow cell consisting of crossed channels that are  $650 \mu\text{m}$  wide and  $500 \mu\text{m}$  deep (Fig. 1a). Due to the small length scale ( $L=650 \mu\text{m}$ ) the Reynolds number ( $Re$ ) is small ( $Re < 10^{-2}$ ). Here,

$Re = \rho LU / \eta$ , where  $U$  is the RMS velocity,  $\rho$  is the fluid density, and  $\eta$  is the fluid viscosity. For the polymeric fluid, we also define the Deborah number ( $De$ ), which is the product of the longest relaxation time of the fluid ( $\lambda$ ) and the flow strain rate ( $\dot{\epsilon}$ ). The polymer used here is high molecular weight polyacrylamide (PAA,  $18 \times 10^6$  MW), which has a flexible backbone. Solutions are made by adding 200 ppm of PAA to a viscous Newtonian solvent (95%-Glycerol aqueous solution). The solution is considered dilute; the overlap concentration ( $c^*$ ) for PAA solutions is approximately 310 ppm. The fluid is characterized using a stress-controlled rheometer. We find that the PAA solution has shear-viscosity that is nearly constant up to  $10 \text{ s}^{-1}$ . This behavior is typical of Boger fluids [25]. The longest relaxation time of the fluid ( $\lambda$ ) is obtained using a direct measurement of the first normal stress difference ( $N_1$ ). At sufficiently low shear rates,  $N_1$  is nearly proportional to the mean square shear rate  $\dot{\gamma}^2$  and thus the first normal stress coefficient, given by  $\Psi_1 = N_1 / \dot{\gamma}^2$ , approaches a constant value  $\Psi_{1,0}$  at low shear rates. For a Boger fluid, a constant Maxwell relaxation time can be defined as  $\lambda = \Psi_{1,0} / 2\eta$  [26]. We find that  $\lambda = 4.0 (\pm 0.4)$  seconds. Fluorescein dye at concentration  $1 \times 10^{-3} \text{ M}$  can be added for visualization. Fluid is injected into the cross slot geometry using syringe pumps; the flow rate is constant to about 1.0 %.

To demonstrate the first instability, we show the results of dye advection experiments using an epifluorescence microscope in which a blue light illuminates the cross-slot region, where the flow is strongly extensional. (There is also of course some vorticity due to the upper and lower boundaries of the flow channel.) A small quantity of dyed solution (bright) is injected into one inlet, while undyed polymer solution (dark) is injected into the other inlet. Fig. 1(a) shows the results for a Newtonian fluid (99% Glycerol) at  $Re = 0.01$ . The snapshot reveals a sharp interface at the center of the cross-slot region between the dye and undyed fluids, which demonstrates that this fluid does not mix.

Figure 1(b) reveals an entirely different behavior if we replace the Newtonian fluid by the dilute PAA solution. The snapshot of the advected dye pattern at  $De = 1.5$  shows that the interface is deformed (wavy), although still sharp. The pattern is steady and does not change significantly over several minutes. The mirror image of this pattern can also occur, depending on initial conditions. That is, the flow is bistable [27, 28].

We measure velocity fields for these two fluids by tracking small fluorescent particles ( $5 \mu\text{m}$  diameter) in the fluid. Figure 1(c) shows both typical particle paths and the magnitude of the time-independent velocity field of the Newtonian fluid in the cross-slot region: a well-defined symmetric extensional flow. Note that the velocity vanishes at the stagnation point at the center of the cross-slot, where the strain rate is highest, and the fluid is most strongly stretched. The velocity field (Fig. 1d) shows a deformed and asymmetric flow for the PAA solution.

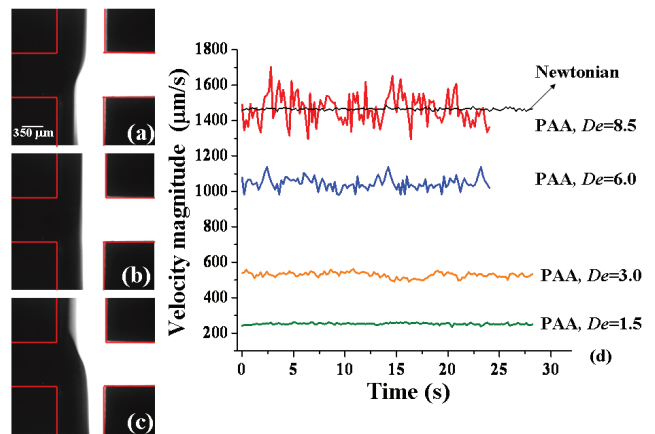


FIG. 2: (Color Online) (a-c) Dye advection patterns for the PAA solution in the time dependent regime ( $De = 8.5$ ) at 1.75 s intervals. (d) Velocity magnitude, averaged over the central 23% of the intersection region, for PAA at various  $De$  and for a Newtonian fluid. The flexible polymer solution becomes time-dependent, but the Newtonian fluid does not.

The flow field for the PAA solution becomes time-dependent when  $De$  is increased beyond 4.0. We illustrate this time dependence by showing a series of dye advection images Fig. 2(a-c) at  $De = 8.5$ . These are consecutive snapshots of dye fields in the cross-slot, taken 1.75 s apart. The dye pattern oscillates, as can be illustrated by considering the interface between the dyed and undyed fluids and following the interface evolution over time. At a given instant, the dyed solution no longer divides itself equally between the two outlets. The interface between the fluids is not as sharp as before (e.g. Fig. 1c). This indicates that the three-dimensional structure is more complex than in the steady case.

To quantify the time dependence of the flow, we sample a small square region in the cross-slot (about 23% of the channel width, centered on the stagnation point), and measure the average speed in that as a function of time. Sampling times are long enough to ensure the accuracy of the velocimetry measurement (10 ms), but are much shorter than the typical timescale of the fluid motion (of order 2 s). Sequences of velocity records for flow at several  $De$  and a Newtonian case are shown in Fig. 2(d). As  $De$  is increased, the speed fluctuations become larger. The Newtonian case produces no such fluctuations at comparable strain rates. We also find no time-dependence with a solution of Xanthan Gum, a semi-rigid polymer (not shown).

The corresponding power spectra of the local velocity records are shown for two values of  $De$  in Fig. 3. Since the entire velocity field must be measured at each time, the velocity records are only a few hundred points long, but this is sufficient to establish the qualitative features of the spectra. The spectral power at low frequencies grows about 2-4 orders of magnitude as  $De$  is increased from

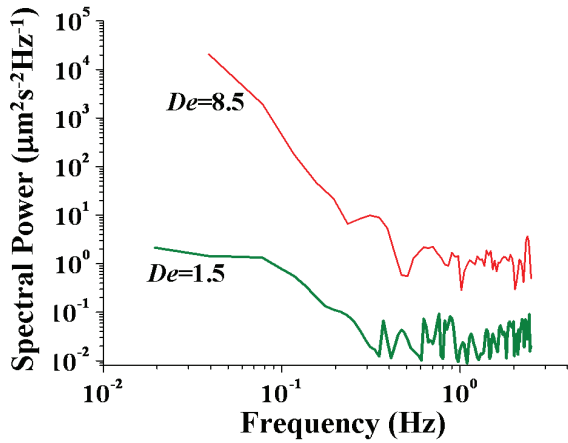


FIG. 3: (Color Online) Corresponding power spectra of the velocity measurements for  $De=1.5$  and  $De=8.5$ . No distinct period is found.

1.5 to 8.5. The velocity fluctuations appear to be non-periodic, with a possible power-law decay. Power spectra for the Newtonian and Xanthan Gum cases are nearly flat (not shown). Power law spectra for other low  $Re$  polymer flow instabilities have also been demonstrated [10]. Despite temporal fluctuations in the velocity field, no mixing is observed in the cross-slot region.

Next, we examine the variation of the velocity field with  $De$  in Fig. 4. At low  $De$  ( $De=0.4$ ), the velocity field resembles the Newtonian case in that it is symmetric and steady (Fig. 4a). The developing asymmetry is evident at  $De=1.5$ , but the flow remains steady (Fig. 4b). As the  $De$  is further increased to 8.5, we note the appearance of vortices, as shown in Figure 4(c). These vortices fluctuate in space and time, rendering the velocity field time-dependent. We estimate the onset of time dependence to occur approximately at  $De=4.0$ . Flow asymmetry and time-dependent velocity fields have also been reported in macroscopic entry flows at higher  $Re$ , and have been related to the extensional properties of the fluid [8]. Recently, qualitative similar behavior has been observed in entry flows of low-viscosity elastic fluids in microchannels [27, 28] using streak imaging methods; velocity fields were not reported.

We characterize the distortion quantitatively by computing the root-mean-square deviation of the velocity field from the Newtonian case at the same shear-rate, and using this quantity as an order parameter. The velocity fields are first normalized by their respective means:  $\tilde{\vec{V}} = \vec{V}(x, y) / \langle \vec{V}(x, y) \rangle$ . We then compute the RMS difference  $\Delta\tilde{V}_{RMS} = \langle (\tilde{\vec{V}}_P - \tilde{\vec{V}}_N)^2 \rangle^{0.5}$ , where  $\vec{V}_P$  and  $\vec{V}_N$  are the polymer and Newtonian velocity fields, respectively. We plot the values of  $\Delta\tilde{V}_{RMS}$  as a function of  $De$  in Figure 4(d). The difference is close to zero for low  $De$ , where that velocity fields are nearly identical to their Newtonian counterparts. As  $De$  is increased, we compare the growth of  $\Delta\tilde{V}_{RMS}$  to the square root behavior that

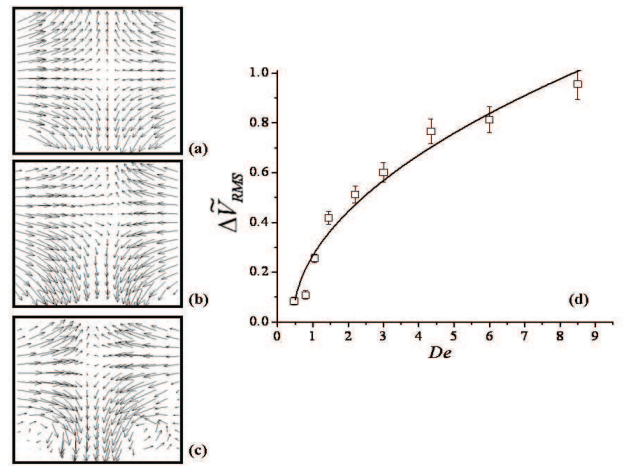


FIG. 4: Velocity fields at (a)  $De=0.4$  (steady), (b)  $De=1.5$  (steady and asymmetric), and (c)  $De=8.5$  (time-dependent and asymmetric). (d) Normalized RMS deviation  $\Delta\tilde{V}_{RMS}$  of PAA velocity fields from the Newtonian case at the same shear-rate (see text), along with a fit to the expected square root law for a normal bifurcation.

is typical of forward bifurcations. The fit is reasonable even above  $De=4.0$ , where the flow is time-dependent. We find that the critical  $De$  is  $0.59 (\pm 0.06)$ , which is close to the predicted value of  $0.5$  [19].

This departure from Newtonian behavior as  $De$  is increased presumably corresponds to the 'coil-stretch' transition of the individual polymer molecules. We do not find significant hysteresis in the measured order parameter for this instability. This is puzzling since the microscopic transition does show hysteresis.

Although Poiseuille flows of viscoelastic fluids are linearly stable (due to the lack of curved streamlines), the elastic instability near the hyperbolic point of the microchannel strongly perturbs the downstream Poiseuille flow. We demonstrate this fact by plotting in Fig. 5(a) the normalized speed as a function of the transverse channel coordinate, 15 channel diameters downstream from the hyperbolic point. The velocity profile for a Newtonian fluid shows the familiar parabolic profile. This is also the case for a PAA solution at  $De=0.4$  (below the instability threshold). However, at higher  $De>4.0$ , e.g. at  $De=8.5$ , we find that the velocity profile is asymmetric and time-dependent even far downstream.

Achieving efficient mixing in microchannels is not a trivial task because the flow is inherently laminar ( $Re<1$ ) due to small length scales. Several methods have been proposed based on temporal [29] or spatial [30] forcing of the flow, 3D [31] and curved geometries in conjunction with dilute polymer solutions [11]. The instabilities documented here can also promote mixing in a simple steadily-forced flow. By inserting an extra "T" at each outlet as shown in Fig. 5(b), we find that the extensional flow instabilities cause stretching and folding of fluid elements in the outlet region. This is demonstrated in Fig

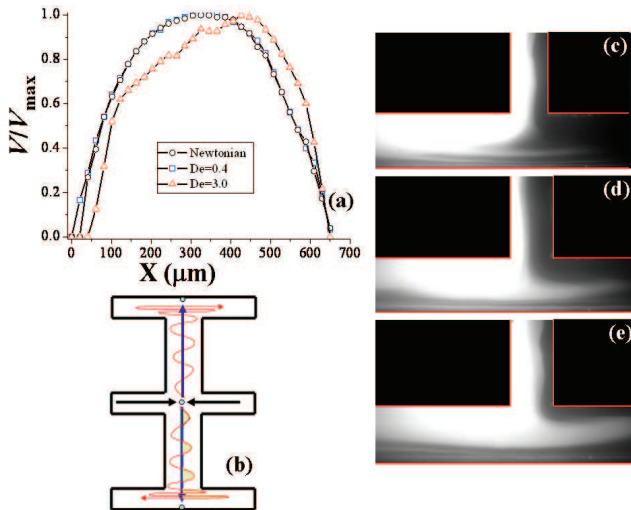


FIG. 5: (Color Online) (a) Longitudinal velocity (normalized by the maximum value) as a function of the cross-channel coordinate at 15 particle diameters downstream of the hyperbolic point, showing the strong distortion caused by the first instability. (b) Modified apparatus with an extra "T" at each outlet to promote mixing. (c-e) Dye snapshots showing the stretching and folding of fluid elements in one of the end regions that results from the time-dependent instability, at  $De=8.5$ .

5(c-e), where we show snapshots taken 0.5 s apart. Here, the instability in the cross-slot leads to distorted regions

of dyed and undyed fluid that are transported to the extra "T" at the end, where they are stretched and folded as illustrated schematically in Fig. 5(b).

In conclusion, we find that flexible polymer solutions show two distinct instabilities in a low  $Re$  ( $<0.01$ ) extensional flow. The first at  $De=0.6$  leads to spatial symmetry-breaking and bistability, while the second at  $De=4.0$  produces broadband temporal fluctuations. We hypothesize that these instabilities are controlled by the stretching of polymer molecules near the hyperbolic point. This view is supported by numerical simulations [14, 16], birefringence measurements [20, 21], and direct measurements of DNA molecules [13, 24], which have shown molecule extension in a cross-channel flow above a critical strain rate. In addition, the instabilities observed here are likely connected to the extensional properties of the fluid, which have been shown to affect flow behavior in entry flows [8]. Given the clear evidence presented here that the initial instability is a forward bifurcation, it should be possible to obtain insight into its origin by analysis or computation.

#### Acknowledgments

This work was supported by NSF DMR-0405187. We appreciate helpful conversations with G. Leal, A. Morozov, and W. van Saarloos.

- 
- [1] R. H. Thomas and K. Walters, *J. Fluid Mech.* 18, 33 (1964).
- [2] A. B. Metzner and J. L. White, *AIChE J.* 11, 989 (1965).
- [3] H. Giesekus, *Rheol. Acta* 5, 239 (1966).
- [4] J. V. Lawler, S. J. Muller, R. A. Brown, et al., *J. N-Newt. Fluid Mech.* 20, 51 (1986).
- [5] D. V. Boger, *Annu. Rev. Fluid Mech.* 19, 157 (1987).
- [6] G. H. McKinley, W. P. Raiford, R. A. Brown, et al., *J. Fluid Mech.* 223, 411 (1991).
- [7] E. S. G. Shaqfeh, *Annu. Rev. Fluid Mech.* 28, 129 (1996).
- [8] J. P. Rothstein and G. H. McKinley, *J. N-Newt. Fluid Mech.* 98, 33 (2001).
- [9] R. G. Larson, E. S. G. Shaqfeh, and S. J. Muller, *J. Fluid Mech.* 218, 573 (1990).
- [10] A. Groisman and V. Steinberg, *Nature* 405, 53 (2000).
- [11] A. Groisman and V. Steinberg, *Nature* 410, 905 (2001).
- [12] D. E. Smith, H. P. Babcock, and S. Chu, *Science* 283, 1724 (1999).
- [13] T. T. Perkins, D. E. Smith, and S. Chu, *Science* 276, 2016 (1997).
- [14] T. Hofmann, R. G. Winkler, and P. Reineker, *Phys. Rev. E* 61, 2840 (2000).
- [15] G. H. McKinley and T. Sridhar, *Annu. Rev. Fluid Mech.* 34, 375 (2002).
- [16] C.-C. Hsieh, S. J. Park, and R. G. Larson, *Macromolecules* 38, 1456 (2005).
- [17] P. G. De Gennes, *J. Chem. Phys.* 60, 5030 (1974).
- [18] E. J. Hinch, in *Proceedings Colloques Internationaux du Centre de la Recherche Scientifique (CNRS, Paris, France, 1974)*, p. 241.
- [19] R. G. Larson and J. J. Magda, *Macromolecules*
- [20] G. G. Fuller and G. Leal, *Rheol. Acta* 19, 580 (1980).
- [21] A. Keller and J. A. Odell, *Colloid. Polym. Sci.* 263, 181 (1985).
- [22] R. E. Evans and K. Walters, *J. N-Newt. Fluid Mech.* 20, 11 (1986).
- [23] D. E. Smith and S. Chu, *Science* 281, 1335 (1998).
- [24] C. M. Schroeder, H. P. Babcock, E. S. G. Shaqfeh, et al., *Science* 301 (2003).
- [25] D. V. Boger, *J. Non-Newt. Fluid Mech.* 3, 87 (1977).
- [26] R. B. Bird, C. F. Curtiss, R. C. Armstrong, et al., *Dynamics of Polymeric Liquids: Fluid Mechanics, Vol. 1* (John Wiley & Sons, New York, 1987).
- [27] A. Groisman, M. Enzelberger, and S. R. Quake, *Science* 300, 955 (2003).
- [28] L. E. Rodd, T. P. Scott, D. V. Boger, et al., *J. N-Newt. Fluid Mech.* 129, 1 (2005).
- [29] F. Okkels and P. Tabeling, *Phys. Rev. Lett.*, 038301 (2004).
- [30] A. D. Strook, S. K. W. Dertinger, A. Ajdari, et al., *Science* 295, 647 (2002).
- [31] F. Bottausci, I. Mezic, C. D. Meinhart, et al., *Philos. Trans. Roy. Soc. London A* 362, 1001 (2004).